Journal of Hydrology 532 (2016) 29–36

Contents lists available at ScienceDirect

Journal of Hydrology

journal homepage: www.elsevier.com/locate/jhydrol

A semi-analytical solution for slug tests in an unconfined aquifer considering unsaturated flow ☆

Hongbing Sun *

Department of Geological, Environmental, and Marine Sciences, Rider University, Lawrenceville, NJ, United States

ARTICLE INFO

Article history:
Received 25 July 2015
Received in revised form 16 September 2015
Accepted 19 November 2015
Available online 23 November 2015
This manuscript was handled by Corrado Corradini, Editor-in-Chief, with the assistance of Rao S. Govindaraju, Associate Editor

Keywords:
Slug test
Unsaturated flow
Groundwater

SUMMARY

A semi-analytical solution considering the vertical unsaturated flow is developed for groundwater flow in response to a slug test in an unconfined aquifer in Laplace space. The new solution incorporates the effects of partial penetrating, anisotropy, vertical unsaturated flow, and a moving water table boundary. Compared to the Kansas Geological Survey (KGS) model, the new solution can significantly improve the fittings of the modeled to the measured hydraulic heads at the late stage of slug tests in an unconfined aquifer, particularly when the slug well has a partially submerged screen and moisture drainage above the water table is significant. The radial hydraulic conductivities estimated with the new solution are comparable to those from the KGS, Bouwer and Rice, and Hvorslev methods. In addition, the new solution also can be used to examine the vertical conductivity, specific storage, specific yield, and the moisture retention parameters in an unconfined aquifer based on slug test data.

1. Introduction

Slug test is one of the most important methods and the most common technique for estimating hydraulic conductivity in a groundwater study. For estimations of the hydraulic conductivity by fittings of the modeled to the measured hydraulic heads in a slug test, three-dimensional solution developed by Hyder et al. (1994), which is also the basis of the popular Kansas Geology Survey (KGS) model, is the most used method. Malama et al. (2011) provided an alternative three dimensional solution considering a moving water table boundary and the inertial effect. For simple estimation of the radial hydraulic conductivity, two dimensional methods by Hvorslev (1951), Cooper, Bredehoeft and Papadopulos (CBP) (Cooper et al., 1967), Dagan (1978), and the Bouwer and Rice (1976; Bouwer, 1989) are still considered the most popular methods, due to their easy usage. Discussions by Chirlin (1989), Chapuis (1998) and Butler (1998) summarized the theories underlying those classical methods. During recent years, sensitivity analyses of the effects of hydraulic parameters on the conductivity estimations in a slug test, including the storativity and vertical anisotropy have been conducted. They have resulted in many valuable recommendations for improving the procedures of data collection and analyses of a slug test (Butler, 1996, 1998; Butler and Healey, 1998; Butler et al., 1994, 1996; Hyder and Butler, 1995; McElwee et al., 1995a,b; Zurbuchen et al., 2002). Relatively, the effect of unsaturated flow on the hydraulic head in a slug test has been largely ignored due to its complexity and the assumption that influence of unsaturated flow could be neglected in the analyses of unconfined tests because of the small time scale involved (Butler, 1998; Weeber and Narasimhan, 1997; Stanford and McElwee, 2000). However, it is now generally accepted that there are two components in the flow of an unconfined aquifer: an instantaneous component to account for aquifer compressibility and a non-instantaneous component for slow drainage from the unsaturated zone of the aquifer (Mathias and Butler, 2006; Moench, 2008). Inclusions of the unsaturated flow in pumping tests have been proven to significantly improve the fitting accuracy between the analytical and the measured hydraulic heads (Moench, 2003, 2008; Mathias and Butler, 2006; Nwankwor et al., 1992; Tartakovsky and Neuman, 2007; Mishra and Neuman, 2010, 2011). The current study will attempt to prove that fitting accuracy between the modeled and measured hydraulic heads for the late stage of a slug test can be significantly improved when the unsaturated flow and delayed yield are considered.

Hence, the objective of this paper is to derive a semi-analytical model that can improve the fittings of the modeled hydraulic

☆ Note: The FORTRAN source code, executable program, and input examples developed for this paper can be downloaded from this URL address: http://users.rider.edu/~hsun/slug9src.htm. It can also be obtained from the author by e-mail.

* Tel.: +1 609 896 5185; fax: +1 609 895 5782.
E-mail address: hsun@rider.edu

http://dx.doi.org/10.1016/j.jhydrol.2015.11.029
0022-1694/

Notation

Most of the dimensionless parameters were defined in Table 1, where a notation with a subscript D and a subscript 1 stand for a standardized and linearized parameter. The remaining dimensionless parameters were defined by their corresponding equations in the text.

a_c	moisture retention exponent (L^{-1})
a_k	relative conductivity exponent (L^{-1})
b	thickness of the saturated aquifer (L)
$c(\psi)$	specific moisture capacity at pressure ψ (L^{-1})
d	upper depth of the well screen (L)
d_s	skin thickness, and average well skin (L)
h	hydraulic head outside the slug well (L)
h_s	average well skin head (L)
$H(0)$, H	initial hydraulic head inside the slug well (L)
$H(t)$	water level in the slug well at time t (L)
I_o	zero-order modified Bessel function's first kind
K_o	zero-order modified Bessel function's second kind
K_r	hydraulic conductivity in the radial direction (L/T)
K_s	hydraulic conductivity of the well skin (L/T)
K_z	hydraulic conductivity in the vertical direction (L/T)
$k(\psi)$	relative conductivity at pressure ψ (dimensionless)
l	lower depth of the well screen (L)
m	thickness of the unsaturated aquifer (L)
p_1, p	Laplace time
r	radial distance away from the slug well (L)
r_c	the radius of the well case (L)
r_w	the effective radius of the well screen (L)
S_s	specific storage coefficient (L^{-1})
S_y	the specific yield (dimensionless)
t	time since the beginning of an instantaneous slug displacement (T)
z	elevation relative to the reference free surface (L)
$\theta(\psi)$	moisture water content at pressure ψ
θ_r	residual moisture water content
ψ_s	pressure head at which the aquifer starts to desaturate/ air entry pressure (L)
η	elevation of the free surface (top of the capillary fringe) (L)
ϕ	hydraulic head in the unsaturated zone (L)
ψ	pressure head (L)
μ	screen length ($l - d$) (L)
$\mathcal{U}(z)$	step function (=1 at $-l \le z \le -d$; =0 at all other z values)

head to the measured head in a slug test that incorporates the unsaturated flow of a finite thickness to allow moisture capacity and relatively conductivity consideration, in addition to the consideration of aquifer compressibility. The derived model considered the linearized unsaturated Richards' equation (1931) following the work of Mathias and Butler (2006) and Kroszynski and Dagan (1975)'s approaches. The solution was obtained in Laplace space and was inverted numerically by de Hoog et al. (1982)'s algorithm. The applicability of the new solution was demonstrated by its applications to the hydraulic heads of slug tests from Houston and Braun (2004) at the Fort Worth, Texas site. The new solution extends the KGS's model (Hyder et al., 1994) and Malama et al. (2011)'s moving water boundary model to include the vertical unsaturated flow. It significantly improved the fittings of the analytical to the measured hydraulic heads during the late stage of a slug test when the unsaturated drainage is significant. The new solution can also be used to analyze the unsaturated moisture parameters and specific yield from a slug test in an unconfined aquifer.

2. Theory

2.1. Mathematical model

The governing equation representing an axisymmetric groundwater flow to a partially penetrating slug well in a compressible, anisotropic, and unconfined aquifer can be written as (Butler, 1998; Hyder et al., 1994):

$$\frac{\partial^2 h}{\partial r^2}+\frac{1}{r}\frac{\partial h}{\partial r}+\frac{K_z\partial^2 h}{K_r\partial z^2}=\frac{S_s\partial h}{K_r\partial t} \tag{1}$$

where h is the hydraulic head outside the slug well, r is the radial distance away from the center of the slug well (Fig. 1), t is the time since the beginning of an instantaneous slug displacement, S_s is the specific storage coefficient, z is the elevation/displacement relative to the water table, and K_r and K_z are the hydraulic conductivities in the radial and vertical directions respectively.

Following Mathias and Butler (2006, p.3)'s Eq. (2), setting the "free surface" on top of the capillary fringe and water table at $z = -\eta$, the initial and boundary conditions are:

$$h(r,z,0)=\psi_s \quad r_w<r<\infty \text{ and } -b\le z\le -\eta \tag{2}$$

$$h(\infty,z,t)=\psi_s \quad -b\le z\le -\eta \tag{3}$$

$$\frac{\partial h}{\partial z}(r,-b,t)=0 \tag{4}$$

where ψ_s is the pressure head at which the aquifer starts to desaturate, also called the air entry pressure, η is the elevation of the "free surface" and b is the thickness of the saturated aquifer. The "free surface" is placed on top of the capillary fringe, instead of bottom, to simplify the expressions related to the unsaturated flow.

At the water table $-\eta$, the boundary condition is:

$$\frac{\partial h(r,\eta,t)}{\partial z}=\frac{\partial \phi(r,\eta,t)}{\partial z} \quad z=-\eta \tag{5}$$

where ϕ is the hydraulic head in the unsaturated zone. Notice (5) is a moving water table boundary condition. Eq. (5) implies that the equilibrium profile of soil moisture versus depth, in the unsaturated and nearly saturated zone, moves instantaneously in the vertical

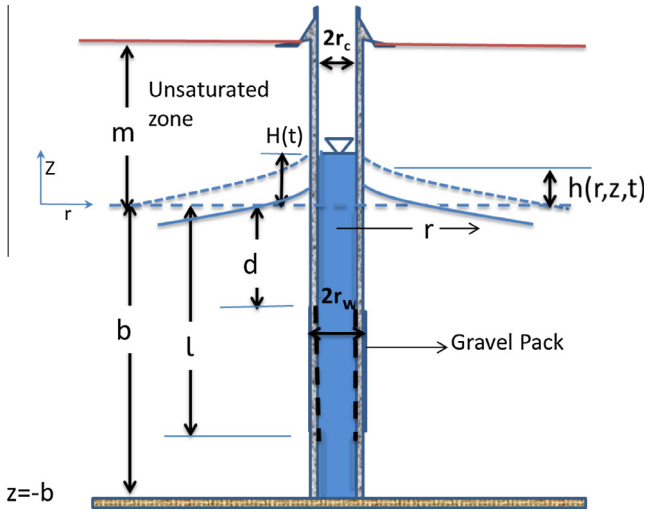

Fig. 1. The component sketch of a well used in the mathematical model of a slug test in an unconfined aquifer.

direction by an amount equal to the change in altitude of the water table.

The initial slug height in the well is:

$$H(0) = H_o \tag{6}$$

where $H(0)$ and H_o are the initial hydraulic head inside the slug well.

The mass balance flow equations for the above, across, and below the well screen between the well and the aquifer are:

$$2\pi r_w K_r d \frac{\partial h(r_w,z,t)}{\partial r} = 0 \quad z \geq -d \tag{7a}$$

$$2\pi r_w K_r (l-d) \frac{\partial h(r_w,z,t)}{\partial r} = \pi r_c^2 \frac{\partial H(t)}{\partial t} \quad -l \leq z \leq -d \tag{7b}$$

$$2\pi r_w K_r (b-l) \frac{\partial h(r_w,z,t)}{\partial r} = 0 \quad z \leq -l \tag{7c}$$

where $H(t)$ is the level of water in the slug well at time t, r_w is the effective radius of the well screen, r_c is the radius of the well case, l and d are the lower and upper depths of the well screen.

Adding the left and right sides of (7a–7c) respectively yields the mass conservation equation between the flow in whole aquifer adjacent to the well screen ($r \to r_w$) and flow in the slug well,

$$2\pi r_w K_r b \frac{\partial h(r_w,z,t)}{\partial r} = \pi r_c^2 \frac{\partial H(t)}{\partial t} \mathcal{U}(z) \tag{7}$$

where $\mathcal{U}(z)$ is a step function, with $\mathcal{U}(z) = 1$ at $-l \leq z \leq -d$ and $\mathcal{U}(z) = 0$ at $z \geq -d$ and $z \leq -l$.

The setup of the well skin effect in a partially penetrating well follows Moench(1997)'s approach for a pumping well in an unconfined aquifer and assumes a linear head distribution across the well skin d_s. The head in the slug well, $H(t)$, is related to the average head in the aquifer adjacent to the slug well screen, h_s, by

$$K_s \frac{(h_s - H(t))}{d_s} = K_r \frac{\partial h(r_w,z,t)}{\partial r} \tag{8}$$

where K_s is the hydraulic conductivity of the well skin, d_s is the skin thickness, and average well skin head h_s is defined as:

$$h_s = \frac{1}{l-d} \int_{-l}^{-d} h(r_w,z,t)dz \tag{8a}$$

Following Mathias and Butler (2006)'s approach, assuming that horizontal unsaturated flow is negligible as compared to vertical unsaturated flow, the Richards (1931) unsaturated flow equation is written as:

$$K_z \frac{\partial}{\partial z}\left(k(\psi)\frac{\partial \phi}{\partial z}\right) = S_y c(\psi) \frac{\partial \phi}{\partial t} \quad \text{where } \phi = \psi + z \tag{9}$$

where S_y is the specific yield, ψ is the pressure head, ϕ is the hydraulic head in the unsaturated zone, $c(\psi)$ and $k(\psi)$ are the specific moisture capacity and relative conductivity respectively. Eq. (9) is subjected to the following initial and boundary conditions:

$$\phi = \psi_s \quad r \geq r_w,\ z \geq -\eta(r,t),\ t = 0 \tag{10}$$

$$\phi = h \quad r \geq r_w,\ z = -\eta(r,t),\ t > 0 \tag{11}$$

$$\frac{\partial \phi}{\partial z} = 0 \quad r \geq r_w,\ z = m,\ t > 0 \tag{12}$$

For $\psi \leqslant \psi_s$,

$$c(\psi) = a_c e^{a_c(\psi - \psi_s)};\ k(\psi) = e^{a_k(\psi - \psi_s)} \tag{13}$$

where a_c is the moisture retention exponent (L^{-1}), a_k is the relative conductivity exponent (L^{-1}), m is the thickness of the unsaturated aquifer, and from Mishra and Neuman (2010, 2011),

$$e^{a_c(\psi-\psi_s)} = \frac{\theta(\psi) - \theta_r}{S_y} \tag{14}$$

where $\theta(\psi)$ is the moisture water content at pressure ψ, and θ_r is the residual moisture water content.

2.2. Standardization and linearization

To simplify the above governing equation and boundary and initial conditions, substitute the dimensionless parameters defined in Table 1 into Eqs. (1)–(13).

Then, following Mathias and Butler (2006)'s (p. 4, Eqs. (17)–(23)) approach, based on the method of Dagan (1978) and Kroszynski and Dagan (1975), assume that the variables can be expanded in perturbation series using ϵ as small parameters:

$$h_D(r_D,z_D,t_D) = \psi_{sD} + \epsilon h_{D1}(r_D,z_D,t_D) + \dots \tag{15a}$$

$$\phi_D(r_D,z_D,t_D) = \psi_{sD} + \epsilon \phi_{D1}(r_D,z_D,t_D) + \dots \tag{15b}$$

$$\psi_D(r_D,z_D,t_D) = -z_D + \psi_{sD} + \epsilon \phi_{D1}(r_D,z_D,t_D) + \dots \tag{15c}$$

$$c_D(\psi_D) = c_{D0} + \epsilon c_{D1} + \dots \tag{15d}$$

$$k_D(\psi_D) = k_{D0} + \epsilon k_{D1} + \dots \tag{15e}$$

$$\eta_D(r_D,t_D) = 0 + \epsilon \eta_{D1}(r_D,z_D,t_D) + \dots \tag{15f}$$

At the water table, $z_D = -\eta_D(r_D,t_D)$, using (15f) and disregarding the higher order terms of ϵ, the dimensionless hydraulic heads of (15a,b) are derived as:

$$h_D(r_D,\eta_D,t_D) = \psi_{sD} + \epsilon h_{D1}(r_D, 0 - \epsilon \eta_{D1}(r_D,t_D) + \dots, t_D) + \dots \tag{16}$$

$$\phi_D(r_D,\eta_D,t_D) = \psi_{sD} + \epsilon \phi_{D1}(r_D, 0 - \epsilon \eta_{D1}(r_D,t_D) + \dots, t_D) + \dots \tag{17}$$

The retaining terms of order ϵ in (16) and (17) are:

$$h_D(r_D,z_D,t_D) = \psi_{sD} + \epsilon h_{D1}(r_D,0,t_D) + O(\epsilon^2) \tag{18}$$

$$\phi_D(r_D,z_D,t_D) = \psi_{sD} + \epsilon \phi_{D1}(r_D,0,t_D) + O(\epsilon^2) \tag{19}$$

From Mathias and Butler (2006), when ϵ is small enough and the second-order terms of ϵ are negligible, this linearization method is valid. Substituting the above ϵ Eqs. (15)–(19) into Eqs. (1)–(12) and only retaining the terms of order ϵ, the set of dimensionless and linearized equations are given as the following. The governing equation is:

$$\frac{\partial^2 h_{D1}}{\partial r_D^2} + \frac{1}{r_D}\frac{\partial h_{D1}}{\partial r_D} + K_D \frac{\partial^2 h_{D1}}{\partial z_D^2} = C_D \frac{\partial h_{D1}}{\partial t_D} \tag{20}$$

The initial and boundary conditions are:

$$h_{D1}(r_D,z_D,0) = 0 \quad 1 < r_D < \infty \tag{21}$$

$$h_{D1}(\infty,z_D,t_D) = 0 \quad t_D > 0 \tag{22}$$

$$\frac{\partial h_{D1}}{\partial z_D}(r_D,-1,t_D) = 0 \quad t_D > 0 \tag{23}$$

Note that now the nonlinear boundary condition at the water table in Eq. (5) can be linearized from the unknown surface $z_D = -\eta_D(r_D,t_D)$ to the horizontal plane $z_D = 0$ (one can picture this transformation as $\eta/b \approx 0$ when $b \gg \eta$).

$$\frac{\partial h_{D1}(r_D,0,t_D)}{\partial z_D} = \frac{\partial \phi_{D1}(r_D,0,t_D)}{\partial z_D} \tag{24}$$

Boundary conditions (6)–(8a) are converted to:

$$H_D(0) = \frac{H_o}{b} = H_{Do} \tag{25}$$

$$\frac{\partial h_{D1}(1,z,t)}{\partial r_D} = \mu_D \frac{\partial H_{D1}(t_D)}{\partial t_D} \mathcal{U}(z_D) \quad -l_D \leq z_D \leq -d_D \tag{26}$$

where $\mu_D = l_D - d_D$ and $\mathcal{U}(z_D) = 1$ at $-l_D \leq z_D \leq -d_D$ and $\mathcal{U}(z_D) = 0$ at $z_D \geq -d_D$ and $z_D \leq -l_D$.

$$H_{D1}(t_D) = h_{sD1} - S_w \frac{\partial h_{D1}(1,z_d,p)}{\partial z_D} \quad -l_D \leq z_D \leq -d_D \tag{27}$$

$$h_{sD1} = \frac{1}{\mu_D} \int_{-l_D}^{-d_D} h_{D1}(r,z,t)dz_D \tag{27a}$$

Table 1
Dimensionless parameters.

$c_D(\psi_D) = c(\frac{\psi}{b}), d_D = \frac{d}{b}, h_D = \frac{h}{b}, H_D = \frac{H}{b}$,
$H_{Do} = \frac{H_o}{b}, k_D(\psi_D) = k(\frac{\psi}{b}), l_D = \frac{l}{b}, m_D = \frac{m}{b}$,
$r_D = \frac{r}{r_w}, r_{wD} = \frac{r_w}{b}, S_w = \frac{K_r d_s}{K_z r_w}, t_D = \frac{2(l-d)K_r t}{r_c^2}, z_D = \frac{z}{b}$,
$\phi_D = \frac{\phi}{b}, \psi_D = \frac{\psi}{b}, \psi_{Ds} = \frac{\psi_s}{b}, \beta_D = \frac{K_z r_c^2}{2S_y K_r (l-d) b}$

Eq. (9) for the governing equation of unsaturated pressure head is converted to:

$$\beta_D \frac{\partial}{\partial z_D}\left(k_{D0}(z_D)\frac{\partial \phi_{D1}}{\partial z_D}\right) = c_{D0}(z_D)\frac{\partial \phi_{D1}}{\partial t_D} \tag{28}$$

where $c_{D0} = c_D(-z_D + \psi_{Ds})$ and $k_{D0} = k_D(-z_D + \psi_{Ds})$ are from (15d) and (15e) when $\epsilon = 0$. The initial and boundary conditions (10)–(12) changes to:

$$\phi_{D1} = 0 \quad r_D \geq 1,\ z_D \geqslant 0,\ t_D = 0 \tag{29}$$
$$\phi_{D1} = h_{D1} \quad r_D \geq 1,\ z_D = 0,\ t_D > 0 \tag{30}$$
$$\frac{\partial \phi_{D1}}{\partial z_D} = 0 \quad r_D \geq 1,\ z_D = m_D,\ t_D > 0 \tag{31}$$

2.3. Laplace transform

The above linearized Eqs. (20)–(31) are subjected to the Laplace transform. The transformed governing equation is:

$$\frac{\partial^2 \bar{h}_{D1}}{\partial r_D^2} + \frac{1}{r_D}\frac{\partial \bar{h}_{D1}}{\partial r_D} + K_D \frac{\partial^2 \bar{h}_{D1}}{\partial z_D^2} = C_D p_1 \bar{h}_{D1} \tag{32}$$

Boundary conditions are:

$$\bar{h}_{D1}(\infty, z_D, p_1) = 0, \tag{33}$$
$$\frac{\partial \bar{h}_{D1}(r_D, -1, p)}{\partial z_D} = 0 \tag{34}$$
$$\frac{\partial \bar{h}_{D1}(r_D, 0, p_1)}{\partial z_D} = \frac{\partial \bar{\phi}_{D1}(r_D, 0, p_1)}{\partial z_D} \tag{35}$$

The transformed equation for (26) is:

$$\frac{\partial \bar{h}_{D1}}{\partial r_D}(1, z_d, p_1) = \mu_D[-H_{Do} + p\overline{H}_{D1}(p_1)]\mathcal{U}(z_D) \tag{36}$$

where $\mathcal{U}(z_D) = 1$ at $-l_D \leq z_D \leq -d_D$ and $\mathcal{U}(z_D) = 0$ at $z_D \geq -d_D$ and $z_D \leq -l_D$.

The transformed equations for (27) and (27a) are:

$$\overline{H}_{D1}(p_1) = \bar{h}_{sD1} - S_w \frac{\partial \bar{h}_{D1}(1, z_d, p_1)}{\partial r_D} \quad -l_d \leq z_d \leq -d_d \tag{37}$$

$$\bar{h}_{sD1} = \frac{1}{\mu_D}\int_{-l_D}^{-d_D} \bar{h}_{D1}(1, z_d, p_1) dz_D \tag{37a}$$

The transformed equation for (28) is:

$$\beta_D \frac{\partial}{\partial z_D}\left(k_{D0}(z_D)\frac{\partial \bar{\phi}_{D1}}{\partial z_{D1}}\right) = p_1 c_{D0}(z_D)\bar{\phi}_{D1} \tag{38}$$

The transformed boundary conditions of (30) and (31) are:

$$\bar{\phi}_{D1} = \bar{h}_{D1} \quad r_D \geq 1,\ z_D = 0 \tag{39}$$
$$\frac{\partial \bar{\phi}_{D1}}{\partial z_{D1}} = 0 \quad r_D \geq 1,\ z_D = m_D \tag{40}$$

3. Analytical solution in Laplace space

Steps for deriving the solution to Laplace transformed governing Eq. (32) using the transformed boundary conditions (33)–(40) are given in the Appendix. The Laplace transformed solution for the dimensionless normalized head considering the well skin effect from (A19) is:

$$\overline{H}_{D1}(p_1) = \frac{H_{Do}[S_w + G]}{1 + p_1[S_w + G]} \tag{41}$$

where

$$G(n) = \frac{1}{\mu_D}\sum_{n=0}^{\infty} \frac{K_0(\lambda_n)[\sin(\varepsilon_n(1-d_D)) - \sin(\varepsilon_n(1-l_D))]^2}{\varepsilon_n^2 \lambda_n K_1(\lambda_n) A(\varepsilon_n)} \tag{42}$$

$\lambda_n = (\varepsilon_n^2 K_D + C_D p_1)^{1/2}$, ε_n is the root of $\varepsilon_n \tan[\varepsilon_n] = q_{uz}(p_1)$, $A(\varepsilon_n)$ from (A12) is:

$$A(\varepsilon_n) = \frac{1}{2} + \frac{\sin(2\varepsilon_n(1-d_D)) - \sin(2\varepsilon_n(1-l_D))}{4\mu\varepsilon_n} \tag{43}$$

$q_{uz}(p_1)$ is obtained from Mathias and Butler (2006)'s Eq. (42),

$$q_{uz}(p_1) = i\left(\frac{a_{Dc}p_1}{\beta}\right)^{1/2}\left\{\frac{J_u[iX(0)] + \alpha Y_u[iX(0)]}{J_v[iX(0)] + \alpha Y_v[iX(0)]}\right\} \tag{44}$$

where $i^2 = -1, X(z_D) = 2\left[\frac{a_{Dc}p_1 e^{(a_{Dk}-a_{Dc})z_D}}{\beta(a_{Dc}-a_{Dk})^2}\right]^{0.5}$, $u = a_{Dc}/(a_{Dc} - a_{Dk})$, $v = a_{Dk}/(a_{Dc} - a_{Dk})$, $\alpha = J_u[iX(m_D)]/Y_u[iX(m_D)]$, $\beta = K_z r_{wD}^2/K_r$, and J_v and Y_v (or subscript u) are the vth-order (or uth-order) Bessel functions of the first and second kind respectively.

The calculation of parameters in $q_{uz}(p_1)$ of Eq. (44) is the same as that of Mathias and Butler (2006)'s Eq. (42) except there is a conversion between the Laplace time p_1 in the current paper and the Laplace time p in their equation where $p_1 = \frac{2r_w^2 \mu_D S_y}{r_c^2} p$.

$H_D(t)$ needs to be obtained by the inverse Laplace transform numerically.

The Laplace transformed solution $\overline{H}_{D1}(p_1)$ for a fully screened aquifer can be obtained by simply setting $d_D = 0$ and $l_D = 1$. The Laplace transformed solution and coefficients to the governing Eq. (41) for the saturated flow only scenario are the same as those for the unsaturated flow shown by Eqs. (41)–(44) except here $\varepsilon_n = (n + \frac{1}{2})\pi$ and there is no need to obtain $q_{uz}(p_1)$.

4. Application

A FORTRAN code was developed to calculate the Laplace transformed hydraulic head from Eqs. (41)–(44). Following Barlow and Moench (2011)'s WTAQ, De Hoog et al. (1982)'s inverse Laplace transform algorithm was used to calculate the normalized hydraulic head of Eq. (1). The applicability of the new solution is examined by comparing the hydraulic heads from the new solution to the measured hydraulic heads of a field site and to the calculated heads from the well-established KGS model (Hyder et al., 1994; Butler et al., 1998) and the Bouwer and Rice model (Bouwer and Rice, 1976).

4.1. Application to field data and comparison with existing models

The new solution was applied to the data of three slug test wells from a site at Fort Worth, Texas. These three slug wells mainly tapped into the poorly sorted unconsolidated alluvial sediments and fill materials. Detailed data regarding the well construction on these three wells can be obtained from Houston and Braun (2004)'s report. Assume that the slug injections were instantaneous (though mechanical slugs were used in their field study), the changes of normalized head at a late stage of these slug tests were due to delayed yield and drainage from the moisture retention, and the effect of a well bore skin is negligible. Both the log time vs. normalized head (H/H_o) and time vs. log normalized head were plotted (Figs. 2 and 3). The log time vs. normalized head plots were to examine the traditional semi-log fittings between the measured

Table 2
Comparison of hydraulic parameters estimated from the new solution and traditional models.

Models\Parameters	K_r (m/day)	K_z (m/day)	S_s (m^{-1})	S_y	a_c (m^{-1})	a_k (m^{-1})
Well ST14-03[a]						
New solution	2.76	2.59	$3.5 * 10^{-5}$	0.1	1.5	150
KGS model	2.06	1.21	$7.52 * 10^{-5}$			
Bouwer & Rice model	2.27					
Hvorslev	2.95					
WSAICTA027[a]						
New solution	2.24	2.16	$5 * 10^{-5}$	0.10	1.2	350
KGS model	2.39	0.286	$6.84 * 10^{-5}$			
Bouwer & Rice model	1.89					
Hvorslev	2.71					
MW-12[a]						
New solution	2.51	2.24	$2 * 10^{-4}$	0.12	0.8	400
KGS model	1.55	1.08	$1.8 * 10^{-3}$			
Bouwer & Rice model	2.01					
Hvorslev	2.85					

[a] Hydraulic heads for slug tests from well ST14-03, WSAICTA027, and MW-12 were obtained from Houston and Braun, USGS.

and modeled heads (Figs. 2a and 3a) for extracting the radial hydraulic conductivity and specific storage coefficient. The heads from the Bouwer and Rice model were not plotted in the log time vs. normalized head plot because the Bouwer and Rice model is a semi-log straight-line fitting model (Bouwer and Rice, 1976). It is clear that normalized hydraulic heads from the new solution can match the measured hydraulic heads well. The radial hydraulic conductivities obtained by the new solution also are comparable to that from the traditional KGS, Bouwer and Rice, and Hvorslev models (Table 2).

The time vs. log normalized head plots (Figs. 2b and 3b) were to demonstrate the improvement in fittings between modeled and the measured hydraulic heads during the late stage of a slug test which are affected more by the unsaturated flow and delayed yield. It also helps the calibration of moisture capacity and relative conductivity exponents and specific yield. The time vs. log normalized head plot amplifies the moisture drainage effect during the late stage of the slug test. It needs to be emphasized that two (WSAICTA027, and MW-12) of the three slug wells have partially submerged screen which allow significant unsaturated drainage above the water table (see Houston and Braun, 2004's Table 4 on p. 11, for details about the well screen) as shown by the measured data. In Figs. 2b and 3b, the results from the new solution have shown excellent fittings to measured data for the late stage of the tests when the unsaturated drainage is important. This improved fitting is a significant improvement over the KGS model. The addition of the unsaturated flow in the new solution also allows the estimation of the specific yield and moisture capacity and relative conductivity exponents during the fitting process (Table 2) which is another advantage over the traditional slug test model.

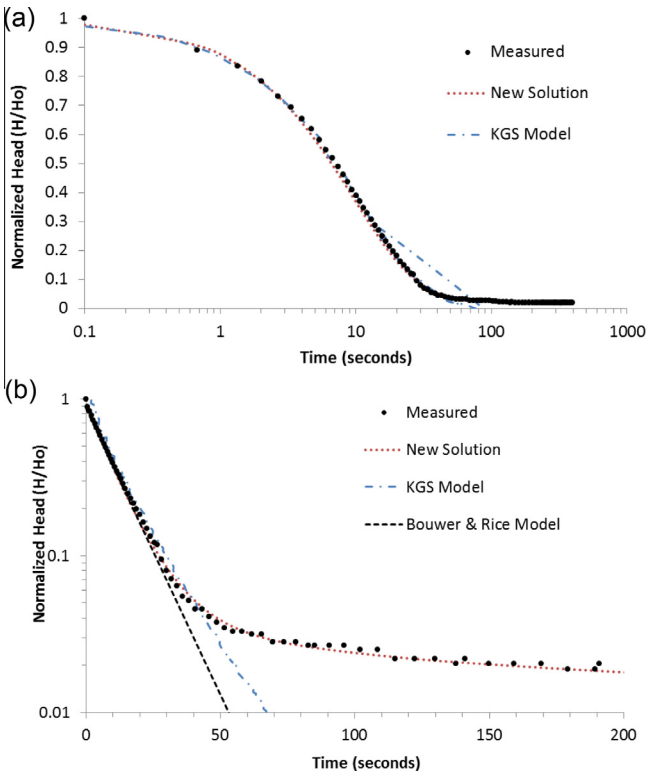

Fig. 2. (a) log time vs. normalized head, (b) time vs. log normalized head plots for well ST14-03 showing the best fit curves from the new solution, the KGS model, and the Bouwer & Rice model to the measured slug test data. Notice the significant improvement of the new solution for fitting the late slug test data which were affected by unsaturated drainage.

4.2. Parameter calibration and sensitivities

During the hydraulic head fittings and the parameter estimations by the new solution in the above examples (Figs. 2 and 3), horizontal (or radial) and vertical conductivities and specific storage were calibrated first because they are the prominent factors. Horizontal conductivity was calibrated by fitting the modeled log time vs. normalized head to that of measured while assigned a fixed initial vertical conductivity and specific storage (Figs. 2a and 3a). Then, the specific storage was calibrated with an assigned vertical conductivity. Finally, the vertical conductivity was calibrated by refining the modeled and measured curvature slopes of log time vs. normalized head plots. The normalized hydraulic head curve at the late stage of the slug test were calibrated by moisture capacity (a_c) and relative conductivity (a_k) exponents, and specific yield using the time vs. log normalized head plot because this semi-log plot amplifies the hydraulic head change in the late stage of a slug test when the unsaturated flow dominates (Figs. 2b and 3b). One can reduce the value of a_c or increase the value of a_K to force the log normalized head vs. time curve to bend more horizontally to match the effect of long unsaturated drainage and delayed yield. The horizontal and vertical hydraulic conductivity and the specific storage were refined at this late stage of calibration as well. Steps for calibrations of the hydraulic parameters will be more obvious after the examinations of their sensitivity plots in the following section.

The values of each hydraulic parameter were varied by a factor of 10 in the sensitivity analyses. It can been seen in Figs. 4–6 that the "Best Fit" curve from the new solution shown an excellent fit to the measured hydraulic head from late stage of the slug test in MW-12 well. For hydraulic heads from the early stage of a slug test

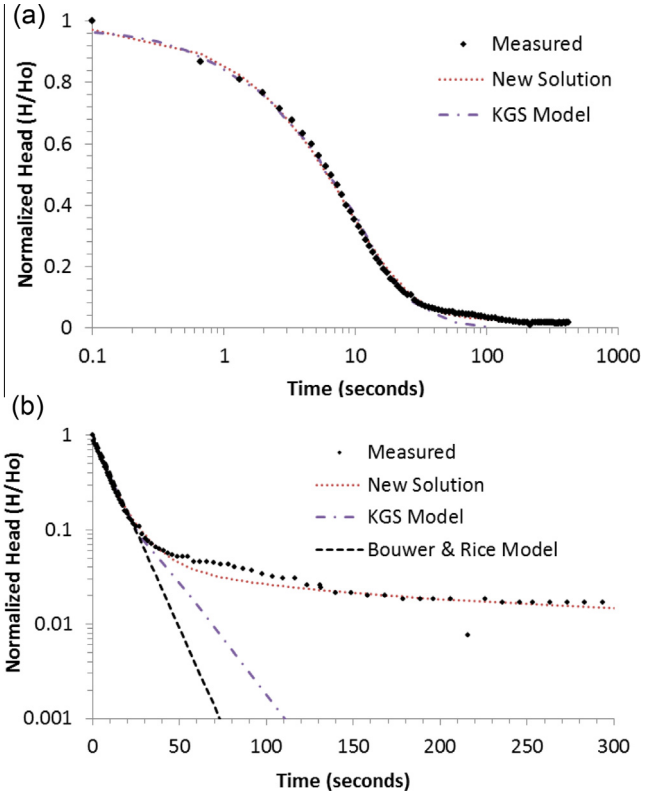

Fig. 3. (a) log time vs. normalized head, (b) time vs. log normalized head plots for well WSAICTA027 showing the best fit curves from the new solution, the KGS model, and the Bouwer & Rice model to the measured data.

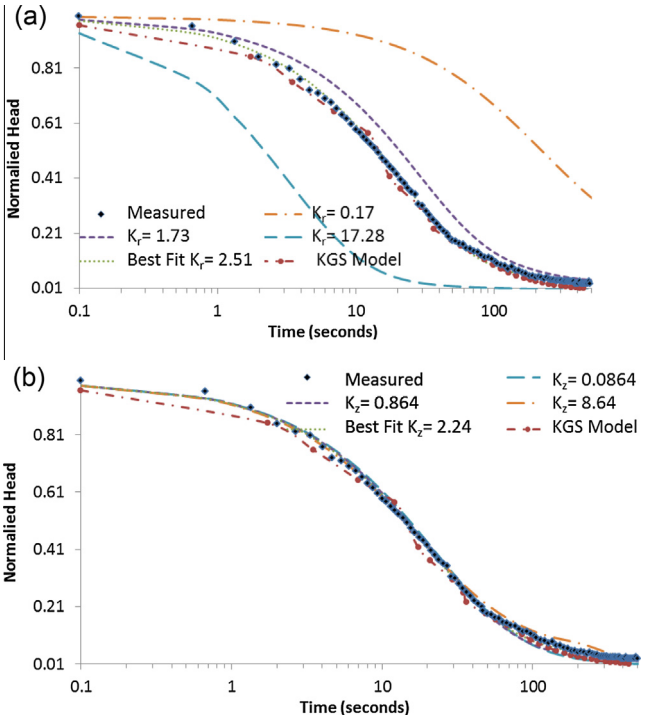

Fig. 4. (a) log time vs. normalized head plots of MW-12 showing the effect of, a, the horizontal conductivity K_r (m/day) and, (b) vertical conductivity K_z (m/day), on the fittings of the hydraulic head from the new solution to the measured data. Values of other parameters are listed in Table 1. Legend marked as "Best Fit K_r = 2.51" curve is the best fit curve from the new solution and will have the same meaning in two late figures.

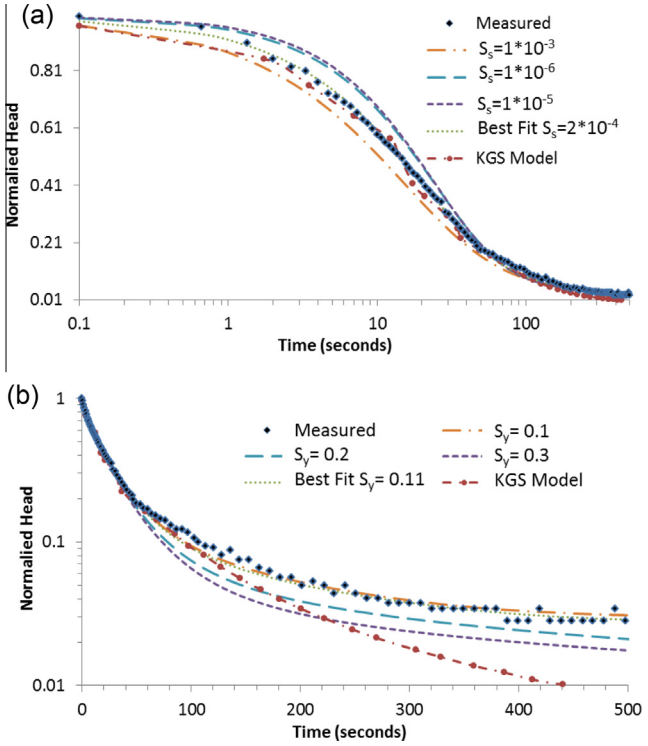

Fig. 5. (a) log time vs. normalized head plot of MW-12 showing the effect of specific storage coefficient (m^{-1}), and (b) time vs. log normalized head plot of MW-12 showing the effect of specific yield, on the curve fittings of the hydraulic head from the new solution to the measured data. Values of other parameters are listed in Table 1.

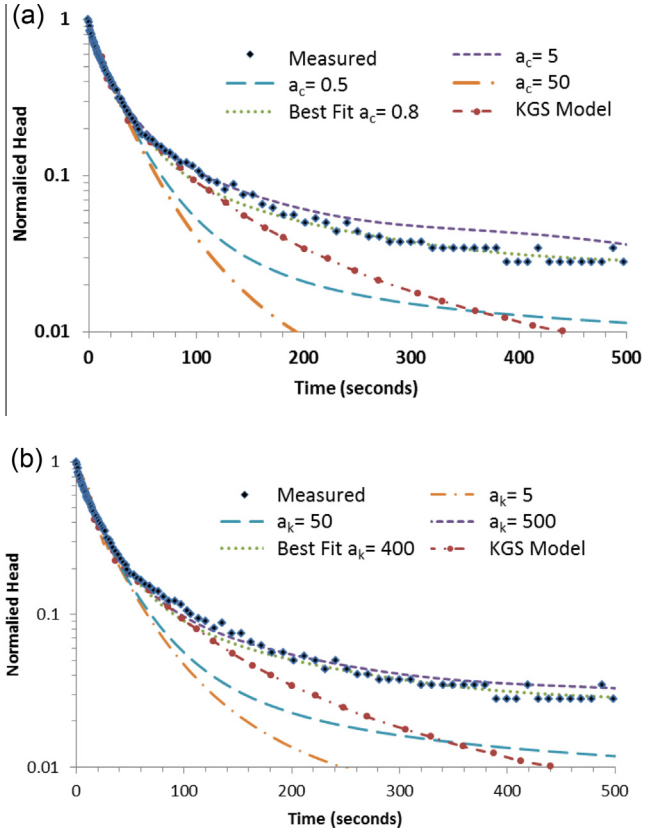

Fig. 6. (a) time vs. log normalized head plots of MW-12 showing the effect of, a, the moisture retention exponent a_c (m^{-1}) and, (b) relative conductivity exponent a_k (m^{-1}), on the fittings of the hydraulic head from the new solution to the measured data. Values of other parameters are listed in Table 1. The KGS model fit is shown as well.

when the saturated flow dominates, changes of the normalized hydraulic head are most sensitive to the changes of the horizontal hydraulic conductivity K_r, and less sensitive to the changes of the specific storage S_s, and least sensitive to the changes of the vertical hydraulic conductivity K_z (Figs. 4 and 5a). The limitation for the parameter estimation in the saturated flow from the new solution is probably similar to that of Hyder et al. (1994)'s solution as discussed by Cardiff et al. (2011). For hydraulic heads from the late stage of a slug test when moisture drainage and delayed yield exist in an unsaturated flow, changes of normalized hydraulic head are sensitive to moisture capacity exponents (a_c), relative conductivity exponents (a_k) and specific yield (S_y) in the new solution (Figs. 5 and 6). Small values of a_c or large values of a_k ($a_c = 5$, $a_k = 500\ \mathrm{m}^{-1}$) relates more to the upward curvature and less gravitational drainage release. Large specific yield correlates to a quick initial reduction in the normalized head (Fig. 5b). In the calibration, one also needs to be careful that a_c and a_k are in reasonable ranges so that moisture exponents bear physical meanings as discussed by other researchers (Mathias and Butler, 2006; Moench, 2008).

5. Conclusions

A new semi-analytical solution considering the Richards' equation for a vertical unsaturated flow was developed for a slug test in the Laplace space. Comparing to traditional models, the new solution significantly improved the fittings of modeled to measured normalized hydraulic heads during the late stage of a slug test when the unsaturated drainage is important. This is apparent for wells with a partially submerged screen where the unsaturated drainage into the aquifer from above water table may be significant. The new solution can be used to estimate and examine the horizontal and vertical hydraulic conductivities, specific storage, the ranges of moisture capacity and relative conductivity exponents, and the specific yield that characterize both the saturated and the unsaturated flow in an unconfined aquifer.

Acknowledgements

The author thanks Natalie Houston and Christopher Braun of US Geological Survey, Austin office for generously providing the original data on the three slug test wells of the Texas site discussed in this paper. The author acknowledges the two anonymous reviewers for their suggestions which helped improve the current text. Finally, the author thanks Andrew Markoe and Jason McCullough of Mathematical Department at Rider University for helping me clear a few basic math concepts and Michael Sun of Johns Hopkins University for his editorial assistance.

Appendix

This appendix provides the derivation for the solution Eqs. (41)–(43). The governing equation was given by Eq. (32). The boundary conditions were given by Eqs. (33)–(37). Following Moench (1997, 1998)'s approach, a solution to (32) that satisfies (34) is given in a form of discrete Fourier transform in the z_D direction with $\bar{f}_n$ as the coefficient:

$$\bar{h}_{D1}(r_D, z_D, p) = \sum_{n=0}^{\infty} \bar{f}_n(r_D, p_1)\cos[\varepsilon_n(z_D+1)] \tag{A1}$$

This setup is also similar to the solution setup by Sun (1997) for groundwater flow in response to a wave boundary condition. The boundary condition (35) adding the solution of unsaturated flow $\bar{q}_{uz}(p_1)$ is:

$$\frac{\partial \bar{h}_{D1}(r_D,0,t_D)}{\partial z_D} = \frac{\partial \bar{\phi}_{D1}(r_D,0,t_D)}{\partial z_D} = -\bar{q}_{uz}(p_1)\bar{h}_{D1}(r_D,0,t_D) \tag{A2}$$

Apply (A1), (A2) and evaluate at $z_d = 0$,

$$-\varepsilon_n \tan\varepsilon_n = -q_{uz}(p_1) \tag{A3}$$

where $q_{uz}(p_1)$ is given in (44) and ε_n is the root of (A3) which can be solved by trial and error method numerically.

Substituting (A1) into (32) gives:

$$\sum_{n=0}^{\infty}\left[\bar{f}_n'' + \frac{1}{r_D}\bar{f}_n' - (\varepsilon_n^2 K_D + C_D p_1)\bar{f}_n\right]\cos[\varepsilon_n(z_D+1)] = 0 \tag{A4}$$

From (A4), the following equation is obtained:

$$\bar{f}_n'' + \frac{1}{r_D}\bar{f}_n' - (\varepsilon_n^2 K_D + C_D p_1)\bar{f}_n = 0 \tag{A5}$$

(A5) is a modified Bessel's differential equation and has the following general solution:

$$\bar{f}_n = C_m I_0(\lambda_n r_D) + C_n K_0(\lambda_n r_D) \tag{A6}$$

where $\lambda_n = (\varepsilon_n^2 K_D + C_D p_1)^{1/2}$, I_o and K_o are the zero-order modified Bessel function's first and second kind, C_m and C_n are coefficients that can be determined from the following procedures.

By applying (33) and letting $C_m = 0$, (A6) is simplified to:

$$\bar{f}_n = C_n K_0(\lambda_n r_D) \tag{A7}$$

Substituting (A7) into (A1) gives:

$$\bar{h}_{D1} = \sum_{n=0}^{\infty} C_n K_0(\lambda_n r_D)\cos[\varepsilon_n(z_D+1)] \tag{A8}$$

Differentiate (A8) over r_D, evaluate at $r_D = 1$, and equal it to (36):

$$\begin{aligned}\frac{\partial \bar{h}_{D1}}{\partial r_D}\Big|_{r_D=1} &= -\sum_{n=0}^{\infty} C_n \lambda_n K_1(\lambda_n)\cos[\varepsilon_n(z_D+1)] \\ &= \mu_D[-H_{Do} + p\bar{H}_{D1}(p_1)]\mathcal{U}(z_D)\end{aligned} \tag{A9}$$

Define $q_s = -H_{Do} + p\bar{H}_{D1}(p_1)$, which is only a function of the Laplace time p_1. Multiplying the right two sides of (A9) by $\cos[\varepsilon_m(z_D+1)]$ and integrating the cosine product over the interval $(-l_D, -d_D)$ when $\mathcal{U}(z_D) = 1$, Eq. (A9) becomes:

$$\begin{aligned}&\sum_{n=0}^{\infty}\frac{C_n\lambda_n K_1(\lambda_n)}{\mu_D}\int_{-l_D}^{-d_D}\cos[\varepsilon_n(z_D+1)] * \cos[\varepsilon_m(z_D+1)]dz_D \\ &= -q_s\int_{-l_D}^{-d_D}\cos[\varepsilon_n(z_D+1)]dz_D\end{aligned} \tag{A10}$$

For the left side of (A10), let

$$z_D = -d_D + z_{D2}(l_D - d_D) = -d_D + \mu z_{D2} \text{ where } \mu_D = l_D - d_D$$

Because of the orthogonal property of the integral of cosine products, only when $n = m$, $\int_{-1}^{0}\cos[\varepsilon_m(\mu z_{D2} - d_D + 1)] * \cos[\varepsilon_n(\mu z_{D2} - d_D + 1)]$ does not equal to zero. Substituting z_{D2} for z_D in the left side of (A10), (A10) becomes:

$$\begin{aligned}&C_n\lambda_n K_1(\lambda_n)\int_{-1}^{0}\cos^2[\varepsilon_n(\mu z_{D2} - d_D + 1)]dz_{D2} \\ &= -q_s\int_{-l_D}^{-d_D}\cos[\varepsilon_n(z_D+1)]dz_D\end{aligned} \tag{A11}$$

Using $\cos^2\alpha = \frac{1}{2} + \frac{1}{2}\cos(2\alpha)$, define $A(\varepsilon_n)$ as:

$$\begin{aligned}A(\varepsilon_n) &= \int_{-1}^{0}\cos^2[\varepsilon_n(\mu z_{D2} - d_D + 1)]dz_{D2} \\ &= \int_{-1}^{0}\{1/2 + 1/2\cos[2\varepsilon_n(\mu z_{D2} - d_D + 1)]\}dz_{D2} \\ &= \frac{1}{2} + \frac{\sin[2\varepsilon_n(1-d_D)] - \sin[2\varepsilon_n(1-l_D)]}{4\mu\varepsilon_n}\end{aligned} \tag{A12}$$

Integrate the right side of (A11) and simplify the result with (A12),

$$C_n\lambda_n K_1(\lambda_n)A(\varepsilon_n) = -q_s\frac{\sin[\varepsilon_n(1-d_D)]-\sin[\varepsilon_n(1-l_D)]}{\varepsilon_n} \tag{A13}$$

Rearrange (A13) for C_n,

$$C_n = -\frac{q_s\{\sin[\varepsilon_n(1-d_D)]-\sin[\varepsilon_n(1-l_D)]\}}{\varepsilon_n\lambda_n K_1(\lambda_n)A(\varepsilon_n)} \tag{A14}$$

Substitute (A14) into (A8). At $r_d = 1$, (A8) is:

$$\begin{aligned}\bar{h}_{D1}|_{r_d=1} &= \sum_{n=0}^{\infty} C_n K_0(\lambda_n)\cos[\varepsilon_n(z_D+1)] \\ &= -q_s\sum_{n=0}^{\infty}\frac{K_0(\lambda_n)\{\sin[\varepsilon_n(1-d_D)]-\sin[\varepsilon_n(1-l_D)]\}\cos[\varepsilon_n(z_D+1)]}{\varepsilon_n\lambda_n K_1(\lambda_n)A(\varepsilon_n)}\end{aligned} \tag{A15}$$

From (37a) and (A15), $\bar{h}_{sD1}(1,z_d,p_1)$ is approximated as the average of the integration of Laplace transformed head over interval $(-l_D, -d_D)$ for z_D:

$$\begin{aligned}&\bar{h}_{sD1}(1,z_d,p_1) \\ &= \frac{-1}{\mu_D}\int_{-l_D}^{-d_D} q_s\sum_{n=0}^{\infty}\frac{K_0(\lambda_n)\{\sin[\varepsilon_n(1-d_D)]-\sin[\varepsilon_n(1-l_D)]\}\cos[\varepsilon_n(z_D+1)]}{\varepsilon_n\lambda_n K_1(\lambda_n)A(\varepsilon_n)}dz_D \\ &= \frac{-q_s}{\mu_D}\sum_{n=0}^{\infty}\frac{K_0(\lambda_n)\{[\sin(\varepsilon_n(1-d_D))]-\sin[\varepsilon_n(1-l_D)]\}^2}{\varepsilon_n^2\lambda_n K_1(\lambda_n)A(\varepsilon_n)} = -q_s G\end{aligned} \tag{A16}$$

where

$$G(n) = \frac{1}{\mu_D}\sum_{n=0}^{\infty}\frac{K_0(\lambda_n)\{\sin[\varepsilon_n(1-d_D)]-\sin[\varepsilon_n(1-l_D)]\}^2}{\varepsilon_n^2\lambda_n K_1(\lambda_n)A(\varepsilon_n)} \tag{A17}$$

Substituting (A16), (A9), and q_s into (37) gives:

$$\begin{aligned}\overline{H}_{D1}(p_1) &= \bar{h}_{sD1}(1,z_d,p_1) - S_w\frac{\partial\bar{h}_{D1}(1,z_d,p_1)}{\partial r_D} = -q_s G - S_w q_s \\ &= -[-H_{Do}+p_1\overline{H}_{D1}(p_1)](S_w+G)\end{aligned} \tag{A18}$$

Rearrange (A18),

$$\overline{H}_{D1}(p_1) = \frac{H_{Do}(S_w+G)}{1+p_1(S_w+G)} \tag{A19}$$

References

Barlow, P.M., Moench, A.F., 2011. WTAQ Version 2—A Computer Program for Analysis of Aquifer Tests in Confined and Water-table Aquifers with Alternative Representations of Drainage from the Unsaturated Zone. U.S. Geological Survey Techniques and Methods 3-B9, 41 pp.

Bouwer, H., 1989. The Bouwer and Rice slug test – an update. Ground Water 27, 304–309.

Bouwer, H., Rice, R.C., 1976. A slug test method for determining hydraulic conductivity of unconfined aquifers with completely or partially penetrating wells. Water Resour. Res. 12, 423–428.

Butler Jr., J.J., 1998. The Design, Performance, and Analysis of Slug Tests. CRC Press.

Butler Jr., J.J., 1996. Slug tests in site characterization; some practical considerations. Environ. Geosci. 3, 154–163.

Butler Jr., J.J., Bohling, G.C., Hyderand, Z., McElwee, C.D., 1994. The use of slug tests to describe vertical variations in hydraulic conductivity. J. Hydrol. 156, 137–162.

Butler Jr., J.J., Healey, J.M., 1998. Relationship between pumping-test and slug-test parameters: scale effect or artifact? Ground Water 36, 305–313.

Butler Jr., J.J., McElwee, C.D., Liu, W.Z., 1996. Improving the quality of parameter estimates obtained from slug tests. Ground Water 34, 480–490.

Cardiff, M., Barrash, W., Thoma, M., Malama, B., 2011. Information content of slug tests for estimating hydraulic properties in realistic, high-conductivity aquifer scenarios. J. Hydrol. 403, 66–82.

Cooper, H.H., Bredehoeft, J.D., Papadopulos, S.S., 1967. Response of a finite-diameter well to an instantaneous charge of water. Water Resour. Res. 3, 263–269.

Chirlin, G.R., 1989. A critique of the Hvorslev method for slug test analysis: the fully penetrating well. Ground Water Monit. Remediat. 9, 130–138.

Chapuis, R.P., 1998. Overdamped slug test in monitoring wells: review of interpretation methods with mathematical, physical, and numerical analysis of storativity influence. Can. Geotech. J. 35, 697–719.

Dagan, G., 1978. A note on packer, slug, and recovery tests in unconfined aquifers. Water Resour. Res. 14, 929–934.

de Hoog, F.R., Knight, J.H., Stokes, A.N., 1982. An improved method for numerical inversion of Laplace transforms. SIAM J. Sci. Stat. Comput. 3, 357–366.

Houston, N.A., Braun, C.L., 2004. Analyses and estimates of hydraulic conductivity from slug tests in alluvial aquifer underlying air force plant 4 and Naval Air Station-Joint Reserve Base Carswell Field, Fort Worth, Texas. USGS Sci. Invest. Report. 2004–5225, 22pp.

Hvorslev, M.J., 1951. Time lag and soil permeability in ground-water observations. Bulletin 36, Waterways Exper. Sta. Corps of Engrs, U.S. Army, Vicksburg, Mississippi.

Hyder, Z., Butler Jr., J.J., McElwee, C.D., Liu, W., 1994. Slug tests in partially penetrating wells. Water Resour. Res. 30, 2945–2957.

Hyder, Z., Butler Jr., J.J., 1995. Slug tests in unconfined formations: an assessment of the Bouwer and Rice technique. Ground Water 33, 16–22.

Kroszynski, U.I., Dagan, G., 1975. Well pumping in unconfined aquifers: the influence of the unsaturated zone. Water Resour. Res. 11, 479–490.

Malama, B., Kuhlman, K.L., Barrash, W., Cardiff, M., Thoma, M., 2011. Modeling slug tests in unconfined aquifers taking into account water table kinematics, wellbore skin and inertial effects. J. Hydrol. 408, 113–126.

Mathias, S.A., Butler, A.P., 2006. Linearized Richards' equation approach to pumping test analysis in compressible aquifers. Water Resour. Res. 42, W06508. http://dx.doi.org/10.1029/2005WR004680.

McElwee, C.D., Bohling, G.C., Butler Jr., J.J., 1995a. Sensitivity analysis of slug tests I: the slugged well. J. Hydrol. 164, 53–67.

McElwee, C.D., Butler Jr., J.J., Bohling, G.C., 1995b. Sensitivity analysis of slug tests II: observation wells. J. Hydrol. 164, 69–87.

Mishra, P.K., Neuman, S.P., 2010. Improved forward and inverse analyses of saturated–unsaturated flow toward a well in a compressible unconfined aquifer. Water Resour. Res. 46, W07508. http://dx.doi.org/10.1029/2009WR008899.

Mishra, P.K., Neuman, S.P., 2011. Saturated–unsaturated flow to a well with storage in a compressible unconfined aquifer. Water Resour. Res. 47 (5), W05, 553.

Moench, A.F., 1997. Flow to a well of finite diameter in a homogeneous, anisotropic water table aquifer. Water Resour. Res. 33, 1397–1407.

Moench, A.F., 1998. Correction to "Flow to a well of finite diameter in a homogeneous, anisotropic water table aquifer" by Allen F. Moench. Water Resour. Res. 34, 2431–2432.

Moench, A.F., 2003. Importance of the vadose zone in analyses of unconfined aquifer tests. Ground Water 42, 223–233.

Moench, A.F., 2008. Analytical and numerical analyses of an unconfined aquifer test considering unsaturated zone characteristics. Water Resour. Res. 44, W06409. http://dx.doi.org/10.1029/2006WR005736.

Nwankwor, G.I., Gillham, R.W., van der Kamp, G., Akindunni, F.F., 1992. Unsaturated and saturated flow in response to pumping of an unconfined aquifer: field evidence of delayed drainage. Ground Water 30, 690–700.

Richards, L.A., 1931. Capillary conduction of liquids in porous mediums. Physics 1, 318–333.

Stanford, K.L., McElwee, C.D., 2000. Analyzing slug tests in wells screened across the water table: a field assessment. Nat. Resour. Res. 9, 111–124.

Sun, H., 1997. A two-dimensional analytical solution of groundwater response to tidal loading in an estuary. Water Resour. Res. 33, 1429–1435.

Tartakovsky, G.D., Neuman, S.P., 2007. Three-dimensional saturated–unsaturated flow with axial symmetry to a partially penetrating well in a compressible unconfined aquifer. Water Resour. Res. 43, W0141. http://dx.doi.org/10.1029/2006WR005153.

Weeber, P.A., Narasimhan, T.N. 1997. Slug test in an unconfined aquifer: a Richards's equation perspective. Ernest Orlando Lawrence Berkeley National Laboratory Report, LBNL-40966, 33 pp.

Zurbuchen, B.R., Zlotnik, V.A., Butler Jr., J.J., 2002. Dynamic interpretation of slug tests in highly permeable aquifers. Water Resour. Res. 38. http://dx.doi.org/10.1016/j.jhydrol.2007.08.018, p. 1025, 1–8.